

# Multijet events in the $k_T$ -factorisation scheme

Stefan Höche<sup>1</sup>, Frank Krauss<sup>1</sup>, Thomas Teubner<sup>2</sup>

<sup>1</sup> Institute for Particle Physics Phenomenology, Durham University, Durham DH1 3LE, UK

<sup>2</sup> Department of Mathematical Sciences, University of Liverpool, Liverpool L69 3BX, UK

**Abstract:** A Markovian Monte Carlo algorithm for multi-parton production in the high-energy limit is proposed and the matching with unintegrated parton densities is discussed.

## 1 Introduction

Hard scattering at hadron colliders is usually described within the framework of collinear factorisation [1, 2]. The full scattering amplitude is factorised into a hard perturbative parton scattering matrix element and process-independent universal parton distribution functions (PDFs), which depend on the flavour of the extracted parton, its energy or light-cone momentum fraction  $x$  w.r.t. the initial hadron, and on the factorisation scale  $\mu_F$ . The choice of this scale is, to some extent, arbitrary. By the inclusion of higher-order corrections the dependence of the cross section on this scale is diminished. At present, PDFs cannot be obtained from first principles due to their essentially non-perturbative origin, but they can be extracted from data, for example through global fits [3, 4, 5]. On the other hand, the evolution of these collinear PDFs with changing factorisation scale can be determined perturbatively. In the collinear factorisation scheme, all initial state partons are on-shell and have zero transverse momenta  $k_\perp = 0$ .

An alternative approach is the framework of  $k_\perp$ - or high-energy factorisation. There, unintegrated PDFs (UPDFs) are convoluted with off-shell matrix elements. The PDFs are unintegrated in terms of the initial partons'  $k_\perp$ . Initially,  $k_\perp$ -factorisation has been formulated for heavy quark production [6, 7, 8]. The approach has been further investigated in other channels, see for instance [9, 10, 11].

The  $k_\perp$ -factorisation has apparent advantages over conventional collinear factorisation: First, in the high-energy limit, i.e. for  $t \ll s$  with  $s$  being large, the QCD cross section for jet production is dominated by gluon exchange diagrams, which diverge in this limit. This divergence is alleviated or even removed by realising that the  $1/t$  divergences in the matrix element can be identified with divergences of the form  $1/k_\perp^2$  and thus using a suitable form of unintegrated PDFs, vanishing fast enough for  $k_\perp \rightarrow 0$ . Second, employing UPDFs means including the leading

logarithmic contribution of higher order corrections to a given process, since the effect of additional QCD radiation is encoded in them [12, 13].

Taking the high-energy limit in a given process is equivalent to the BFKL limit [14, 15], which builds on  $t$ -channel dominance of scattering cross sections and the reggeisation of  $t$ -channel gluons [16]. In the past, there have been various approaches, aiming at a solution of the BFKL dynamics with Monte Carlo methods and thus producing exclusive final states. An approximation, aiming at a correct description of essential features of the BFKL equation and a correct extrapolation to the DGLAP regime, has been proposed in the “Linked Dipole Chain Model” [17, 18]. This model has been implemented in [19]. The scope of this approach is closely related to the CCFM equation [20, 21, 22]. Event generators based on this evolution equation have been presented in [23, 24, 25, 26]. An iterative solution of the pure BFKL equation has been proposed in [27], iterative Monte Carlo solutions in [28, 29]. Later on, this prescription has been extended to next-to-leading logarithmic accuracy [30, 31, 32, 33].

In this paper, a different implementation of  $k_\perp$ -factorisation for the case of multijet production is discussed. Emphasis is put on finding a gauge invariant form of the corresponding expressions and on identifying their matching to unintegrated PDFs derived from conventional collinear ones [34, 35, 36]. It turns out that this in fact can be achieved by working in the high-energy limit, using as basic building blocks splitting functions in the limit  $z \rightarrow 0$ ,<sup>1</sup> in conjunction with a proper reggeisation of all  $t$ -channel propagators. Since four-momentum conservation can explicitly be imposed in a Monte Carlo solution, this approach clearly includes effects beyond the naive leading order BFKL limit.<sup>2</sup> Furthermore, identifying the proba-

<sup>1</sup>In addition to the pure gluonic ladders of the high-energy limit, here also vertices for quark production are included.

<sup>2</sup>As was discussed for example in [37, 38, 39, 32], the implementation of four-momentum conservation and running  $\alpha_s$  effects strongly modifies naive LO BFKL predictions, which were shown to poorly

bilistic interpretation of each emission in the high-energy limit, the Monte Carlo solution has for the first time been implemented as a Markovian approach, similar to conventional parton shower event generators. This enables generation of an a priori arbitrary number of emissions, which is important at high energies, where corrections due to large final state multiplicities are sizable.

The paper is organised as follows: In Sec. 2 the procedure of [34,35,36,40] (KMRW) to generate doubly unintegrated PDFs (DUPDFs) and the corresponding angular ordering constraints are reviewed. In Sec. 3 it is then shown that the leading  $\ln(1/x)$  terms are correctly taken into account. Section 4 contains the description of the Markovian MC procedure to generate event topologies with an a priori undetermined number of final state partons. In Sec. 6 first results are presented and Sec. 7 contains our conclusions.

## 2 Unintegrated parton densities and the KMRW procedure

In this section, the KMRW procedure of constructing unintegrated PDFs from conventional DGLAP PDFs [34,35,36,40] is reviewed. The discussion and notation closely follows [36,40].

In collinear factorisation, where the transverse momenta  $k_\perp$  of incoming partons are taken to be zero, the parton densities obey the DGLAP evolution equation [41,42,43,44], which determines the  $\mu_F$ -dependence at fixed light-cone momenta. This evolution equation resums leading logarithmic parts of higher perturbative orders. In a Monte Carlo formulation, real emission corrections can be implemented as a Markov chain of  $1 \rightarrow 2$  parton splittings [45,46,47]. However, a study of QCD beyond double leading logarithmic order reveals that quantum coherence effects suppress parton emissions in regions of phase space, where the emission angle of the emitted parton is larger than the opening angle of the emitting colour dipole [48,46]. To exemplify this, consider a parton evolution chain in the initial state of a DIS event, as depicted in Fig. 1. If angular ordering is fulfilled, the momenta  $k_i$  of the radiated partons will be distributed such that their angle  $\theta_i$  with respect to the beam direction increases from the incoming proton towards the hard scattering. To investigate the implications of this constraint, it is convenient to start with a Sudakov decomposition of the momenta [49],

$$p_i = x_i P + \tilde{\beta}_i q' - k_{i\perp}, \quad k_i = \alpha_i P + \beta_i q' + k_{i\perp}, \quad (1)$$

where  $P$  is the proton momentum,  $q$  is the photon momentum and  $q' = q + x_B P$ , with  $x_B$  being the Björken  $x$ . In the high-energy limit, the proton mass can be neglected,  $m_p^2 \ll Q^2 = -q^2$ . Hence  $q'^2 = 0$  and in the Breit frame

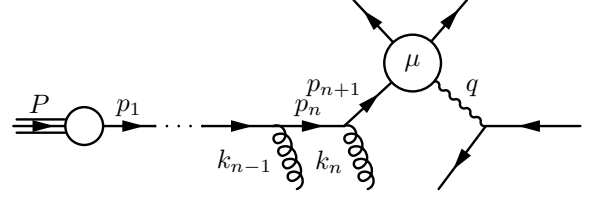


**Fig. 1** Multiple gluon emission in deep inelastic lepton-nucleon scattering. The hard scattering process is characterised by the scale  $\mu$ . Usually this scale is also employed as the factorisation scale.

the momenta read

$$P = \frac{1}{2x_B} (Q, \mathbf{0}, Q),$$

$$q' = \frac{1}{2} (Q, \mathbf{0}, -Q) \quad \text{and}$$

$$k_{i\perp} = (0, \mathbf{k}_{i\perp}, 0).$$

All emitted partons are on-shell, which allows to relate their Sudakov parameters through

$$\beta_i = (\tilde{\beta}_{i-1} - \tilde{\beta}_i) = \frac{z_i}{1 - z_i} \frac{k_{i\perp}^2 / Q^2}{x_i / x_B},$$

where  $z_i = x_i / x_{i-1}$ . Imposing angular ordering for the emissions results in ordering of the corresponding rapidities  $y_i$ , since

$$y_i = \frac{1}{2} \ln \xi_i = -\ln \tan \frac{\theta_i}{2},$$

where  $\xi_i = k_i^+ / k_i^- = \alpha_i / x_B \beta_i$  and  $\theta_i$  is the angle of  $k_i$  with respect to the beam axis. According to Eq. (1)

$$\xi_i = \frac{x_i^2}{x_B^2} \left( \frac{1 - z_i}{z_i} \frac{Q}{k_{i\perp}} \right)^2 = \frac{x_i^2}{x_B^2} \left( \frac{Q}{z_i k_i} \right)^2, \quad (2)$$

where the rescaled transverse momentum  $\bar{k}_i = k_{i\perp} / (1 - z_i)$  has been introduced. Hence angular ordering requirements yield the constraints

$$z_i \bar{k}_i < \bar{k}_{i+1} \quad \text{and} \quad z_n \bar{k}_n < \bar{p}. \quad (3)$$

Here  $\bar{p} = x_{n+1} Q \sqrt{\Xi} / x_B$  is the maximal rescaled transverse momentum which is fixed by the hard process through  $\Xi = (1 + \tilde{\beta}_{n+1}) / (x_{n+1} / x_B - 1)$ . Typically, in an angular ordered evolution of the parton distributions,  $\bar{p}$  plays the role of the factorisation scale  $\mu_F$  [20,21,22,50]. The above ordering procedure can be generalised to hadron-hadron collisions. In this case, both incoming particles have a partonic substructure. In general, this leads to two separate factorisation scales,  $\mu_F^{(1)}$  and  $\mu_F^{(2)}$ , for the two parton densities, respectively.

In [34,35,36,40] it has been shown that doubly unintegrated PDFs (DUPDFs) may be inferred from conventional DGLAP PDFs. In the following, DUPDFs will be

---

describe data.

denoted by  $f_a(x, z, k_\perp^2, \mu_F^2)$ , while their conventional DGLAP counterpart will be denoted by  $f_a(x, \mu_F^2)$ . The DUPDFs must satisfy the normalisation condition

$$\int_x^1 dz \int \frac{dk_\perp^2}{k_\perp^2} f_a(x, z, k_\perp^2, \mu_F^2) = x f_a(x, \mu_F^2). \quad (4)$$

Employing the Sudakov form factor<sup>3</sup>

$$\begin{aligned} \tilde{\Delta}_a(k_\perp^2, \mu_F^2) \\ = \exp \left\{ - \int_{k_\perp^2}^{\mu_F^2} \frac{dk'_\perp^2}{k'^2_\perp} \frac{\alpha_s(k'^2_\perp)}{2\pi} \frac{1}{2} \sum_b \int_0^1 d\zeta \tilde{P}_{ab}(\zeta) \right\}, \end{aligned} \quad (5)$$

with  $\tilde{P}_{ab}(\zeta)$  denoting regularised DGLAP splitting functions for the splitting  $a \rightarrow b$ , a singly unintegrated parton distribution  $\tilde{f}_a(x, k_\perp^2, \mu_F^2)$  is obtained through

$$\tilde{f}_a(x, k_\perp^2, \mu_F^2) = \frac{\partial}{\partial \ln k_\perp^2} \left[ x f_a(x, k_\perp^2) \tilde{\Delta}_a(k_\perp^2, \mu_F^2) \right]. \quad (6)$$

In the region  $k_\perp^2 > \mu_F^2$  this UPDF is set to zero. This procedure leaves some minimum  $k_\perp^2$ -scale to be defined, below which DGLAP parton evolution is not valid. In the following, this scale will be denoted by  $\mu_0^2$ . Relation (6) then holds true only above  $\mu_0^2$ , which yields the constraint

$$\int_0^{\mu_0^2} \frac{dk_\perp^2}{k_\perp^2} \tilde{f}_a(x, k_\perp^2, \mu_F^2) = x f_a(x, \mu_0^2) \tilde{\Delta}_a(\mu_0^2, \mu_F^2)$$

on the singly unintegrated PDF. Whenever UPDFs, satisfying this normalisation condition, are applied in  $k_\perp$ -factorisation, physical observables must be insensitive to details of the infrared behaviour of  $\tilde{f}_a(x, k_\perp^2, \mu_F^2)$ , i.e. below  $\mu_0^2$ .<sup>4</sup> Therefore, a choice can be made, for example [40]

$$\begin{aligned} \tilde{f}_a(x, z, k_\perp^2, \mu_F^2) \Big|_{\mu_F^2 < \mu_0^2} \\ = \frac{k_\perp^2}{\mu_0^2} \left[ A_a(x, z, \mu_F^2) + \frac{k_\perp^2}{\mu_0^2} B_a(x, z, \mu_F^2) \right] \end{aligned}$$

where

$$\begin{aligned} A_a(x, z, \mu_F^2) &= -\tilde{f}_a(x, z, \mu_0^2, \mu_F^2) \\ &\quad + \frac{2x}{1-x} f_a(x, \mu_0^2) \tilde{\Delta}_a(\mu_0^2, \mu_F^2), \\ B_a(x, z, \mu_F^2) &= 2\tilde{f}_a(x, z, \mu_0^2, \mu_F^2) \\ &\quad - \frac{2x}{1-x} f_a(x, \mu_0^2) \tilde{\Delta}_a(\mu_0^2, \mu_F^2). \end{aligned}$$

This choice implies that the UPDF vanishes with  $k_\perp^2 \rightarrow 0$ , as required by gauge invariance [51].

<sup>3</sup> The factor of 1/2 in the sum over the parton species avoids double-counting  $s$ - and  $t$ -channel partons.

<sup>4</sup> It turns out that there is no need for an explicit form of the DUPDFs below  $\mu_0^2$ , since the  $t$ -channel parton chains contain a natural cutoff in  $k_\perp^2$ , cf. [28], by imposing phase space cuts given by physical observables like minijets.

Instead of the regularised splitting functions  $\tilde{P}_{ab}(z)$ , unregularised splitting functions  $P_{ab}(z)$  may safely be used here. This is because the splitting kernels are implicitly regularised by imposing the rapidity ordering constraint Eq. (3). Inserting corresponding  $\Theta$ -functions in  $z$  results in the singly unintegrated quark and gluon distributions  $f_q(x, k_\perp^2, \mu_F^2)$  and  $f_g(x, k_\perp^2, \mu_F^2)$ , respectively [36, 40]. The term singly unintegrated indicates that these PDFs depend on one additional variable w.r.t. the collinear ones. It is straightforward, however, to introduce an additional  $z$ -dependence by simply dropping the  $z$ -integration in Eq. (4). Such defining the DUPDF

$$\begin{aligned} f_a(x, z, k_\perp^2, \mu_F^2) \\ = \Delta_a(k_\perp^2, \mu_F^2) \frac{\alpha_s(k_\perp^2)}{2\pi} \sum_b P_{ba}(z) \frac{x}{z} f_b\left(\frac{x}{z}, k_\perp^2\right) \\ \times \left[ (1 - \delta_{ab}) + \delta_{ab} \Theta\left(\frac{\mu_F}{\mu_F + k_\perp} - z\right) \right] \end{aligned} \quad (7)$$

the desired relation, Eq. (4), is satisfied for both parton species. To guarantee the consistency of the approach, the conventional DGLAP PDF employed to obtain the DUPDFs should be determined using the leading order unregularised splitting kernels employed in Eq. (7). Furthermore, a consistent treatment of the running coupling  $\alpha_s$  should be imposed.

### 3 DUPDFs as impact factors for LL BFKL evolution

In this section we argue that the DUPDFs defined above may be employed as impact factors in the calculation of multi-gluon cross sections in the high-energy limit. The argument works at leading logarithmic (LL) accuracy. The starting point is the integrated LL gluon branching probability  $\Gamma_g^{(LL)} = -\log \Delta_g^{(LL)}$ , which determines the behaviour of the DGLAP evolution of the gluon density.<sup>5</sup>

$$\Gamma_g^{(LL)}(\mu^2, \tilde{\mu}^2) = \Gamma_{gg}^{(LL)}(\mu^2, \tilde{\mu}^2) + \sum_q \Gamma_{gq}^{(LL)}(\mu^2, \tilde{\mu}^2),$$

where

$$\Gamma_{ab}^{(LL)}(\mu^2, \tilde{\mu}^2) = \int_{\ln \mu^2}^{\ln \tilde{\mu}^2} d \ln k_\perp^2 \int_{\frac{k_\perp}{\mu+k_\perp}}^{\frac{\tilde{\mu}}{\tilde{\mu}+k_\perp}} dz \frac{\alpha_s}{2\pi} P_{ab}(z),$$

with  $P_{ab}(z)$  again denoting the unregularised DGLAP splitting kernels and the integration boundaries determined by angular ordering, cf. the  $\Theta$ -function in Eq. (7). To simplify the discussion we firstly focus on  $\Gamma_{gg}^{(LL)}$  only. The corresponding part of the Sudakov form factor reads

$$\Delta_{gg}^{(LL)}(\mu^2, \tilde{\mu}^2) = \exp \left\{ -\Gamma_{gg}^{(LL)}(\mu^2, \tilde{\mu}^2) \right\}.$$

<sup>5</sup> The factor 1/2 contained in Eq. (5) must be cancelled here in order to restore the  $t/u$ -symmetry of the splitting process.

Replacing the splitting variable  $z$  of the emitter parton by the rapidity  $y$  of the emission, which, according to Eq. (2) is given by

$$y = \frac{1}{2} \ln \xi = \ln \left( \frac{x}{x_B} \frac{Q}{k_\perp} \right) - \ln \frac{z}{1-z}$$

results in

$$\begin{aligned} \Gamma_{gg}^{(LL)}(\mu^2, \tilde{\mu}^2) &= - \int_{\ln \mu^2}^{\ln \tilde{\mu}^2} d \ln k_\perp^2 \int_{y(z_{\min})}^{y(z_{\max})} dy \\ &\quad \times \frac{2C_A (1-z(1-z))^2}{P_{gg}(z)} \frac{\alpha_s}{2\pi} P_{gg}(z) \\ &= \int_{\ln \mu^2}^{\ln \tilde{\mu}^2} d \ln k_\perp^2 \int_{y(z_{\max})}^{y(z_{\min})} dy \tilde{\alpha}_s (1-z(1-z))^2, \end{aligned} \quad (8)$$

where  $\tilde{\alpha}_s = \alpha_s C_A / \pi$ . The term  $z(1-z)$  in the numerator corresponds to helicity non-conserving configurations in the  $1 \rightarrow 2$  parton splittings and thus in the impact factor [52]. These configurations are absent in the high-energy limit, which simplifies the integrand of Eq. (8), such that the part of the integrated LL gluon branching probability induced by  $g \rightarrow gg$  splittings reads

$$\Gamma_{gg}^{(LL)}(\mu^2, \tilde{\mu}^2) = \int_{\ln \mu^2}^{\ln \tilde{\mu}^2} d \ln k_\perp^2 \int_{y(z_{\max})}^{y(z_{\min})} dy \tilde{\alpha}_s. \quad (9)$$

Keeping in mind that  $\tilde{\alpha}_s$  depends on transverse degrees of freedom only, performing the  $y$ -integration results in

$$\begin{aligned} \Gamma_{gg}^{(LL)}(\mu^2, \tilde{\mu}^2) &= \int_{\ln \mu^2}^{\ln \tilde{\mu}^2} d \ln k_\perp^2 \tilde{\alpha}_s \\ &\quad \times \left\{ \ln \left( \frac{\tilde{\mu}}{k_\perp} \frac{xQ}{x_B k_\perp} \right) - \ln \left( \frac{k_\perp}{\tilde{\mu}} \frac{xQ}{x_B k_\perp} \right) \right\} \\ &= \frac{1}{2} \int_0^{\ln^2 \tilde{\mu}^2 / \mu^2} d \ln^2 \frac{\tilde{\mu}^2}{k_\perp^2} \tilde{\alpha}_s. \end{aligned}$$

The order of integration in Eq. (9) may be changed,

$$\begin{aligned} \Gamma_{gg}^{(LL)}(\mu^2, \tilde{\mu}^2) &= \int_y^{\tilde{y}} dy' \int_0^{\ln \tilde{\mu}^2 / \mu^2} d \ln \frac{\tilde{\mu}^2}{k_\perp^2} \tilde{\alpha}_s \\ &\quad \times \Theta(\ln \tilde{\mu}^2 / k_\perp^2 + y - y'), \end{aligned} \quad (10)$$

where  $\tilde{y} = \ln x/x_B + \ln Q/\tilde{\mu}$  and  $\tilde{y} - y = \ln \tilde{\mu}^2 / \mu^2$ .

If the running coupling is treated identically, this result agrees with the reggeisation factor of the  $t$ -channel gluon propagator found by rewriting Eq. (7) of [28]. Up to a

minor transformation, this equation reads<sup>6</sup>

$$\begin{aligned} f^n(y_{ab}, p_{a\perp}, p_{b\perp}) &= \int \prod_{i=1}^n \left[ \bar{\alpha}_s dy_i \frac{dk_{i\perp}^2}{k_{i\perp}^2} \frac{d\phi_i}{2\pi} \exp \left\{ -\bar{\alpha}_s \ln \frac{q_{i\perp}^2}{\mu_0^2} \Delta y_i \right\} \right] \\ &\quad \times \exp \left\{ -\bar{\alpha}_s \ln \frac{q_{0\perp}^2}{\mu_0^2} \Delta y_0 \right\} \frac{1}{2} \delta(p_{b\perp} + q_{n\perp}), \end{aligned} \quad (11)$$

where  $\bar{\alpha}_s = \alpha_s C_A / \pi$  and  $q_i = p_a - \sum_{j=1}^i k_j$ . The exponential term in the square brackets is readily identified as

$$\bar{\Delta}(y, \tilde{y}) = \exp \left\{ -\bar{\Gamma}_g^{(LL)}(y, \tilde{y}) \right\}, \quad (12)$$

where

$$\bar{\Gamma}_g^{(LL)}(y, \tilde{y}) = \int_y^{\tilde{y}} dy' \int_0^{\ln q_\perp^2 / \mu_0^2} d \ln \frac{q_\perp^2}{k_\perp^2} \bar{\alpha}_s,$$

which is the desired result. It has been pointed out e.g. in [13] that the comparison with NLO BFKL calculations suggests the choice  $\alpha_s = \alpha_s(k_\perp^2)$ , similar to the DGLAP case. Employing

$$\alpha_s(k_\perp^2) = \frac{1}{\beta_0 \log k_\perp^2 / \Lambda^2}, \quad \text{where} \quad \beta_0 = \frac{11 - 2/3N_f}{4\pi},$$

we then end up with the result presented in [29],

$$\bar{\Gamma}_g^{(LL)}(y, \tilde{y}) = (\tilde{y} - y) \frac{C_A}{\pi \beta_0} \log \left( \frac{\alpha_s(\mu_0^2)}{\alpha_s(q_\perp^2)} \right).$$

In our numerical analyses,  $\Lambda$  is chosen consistent with the input PDF. Equation (11) can be used to construct the full LL BFKL kernel  $f$  through

$$f(y_{ab}, p_{a\perp}, p_{b\perp}) = \sum_{n=0}^{\infty} f^n(y_{ab}, p_{a\perp}, p_{b\perp}). \quad (13)$$

Since rapidity ordering is trivially satisfied in the BFKL evolution, the explicit ordering requirement incorporated in the  $\Theta$ -function of Eq. (10) may be dropped whenever  $\bar{\Delta}(y, \tilde{y})$  is employed.

Following the same reasoning,  $\Gamma_{gq}^{(LL)}$  is given by

$$\begin{aligned} \Gamma_{gq}^{(LL)}(\mu^2, \tilde{\mu}^2) &= \int_{\ln \mu^2}^{\ln \tilde{\mu}^2} d \ln k_\perp^2 \int_{y(z_{\max})}^{y(z_{\min})} dy \tilde{\alpha}_s \\ &\quad \times \frac{T_R}{C_A} \frac{1}{2} z(1-z) (z^2 + (1-z)^2). \end{aligned}$$

In principle, this term vanishes in the high-energy limit due to the prefactor  $z(1-z)$ , thus allowing to identify  $\bar{\Delta}(y, \tilde{y})$  with  $\Delta_g^{(LL)}(\mu^2, \tilde{\mu}^2)$ . However, it may be used to model quark production along the BFKL ladder, as will be discussed in Sec. 5.

<sup>6</sup>Note that the particle indices  $a$  and  $b$  are interchanged with respect to Schmidt's original formulation.

Similar considerations may be applied to the integrated quark branching probability. Starting from the expression

$$\Gamma_q^{(LL)}(\mu^2, \tilde{\mu}^2) = \Gamma_{qg}^{(LL)}(\mu^2, \tilde{\mu}^2) + \Gamma_{qq}^{(LL)}(\mu^2, \tilde{\mu}^2)$$

and again replacing the splitting variable  $z$  by the rapidity  $y$  results in

$$\begin{aligned} \Gamma_{qg}^{(LL)}(\mu^2, \tilde{\mu}^2) &= \int_{\ln \mu^2}^{\ln \tilde{\mu}^2} d \ln k_{\perp}^2 \int_{y(z_{\max})}^{y(z_{\min})} dy \\ &\times \tilde{\alpha}_s \frac{C_F}{2C_A} (1-z) (1+(1-z)^2). \end{aligned}$$

By identifying  $z = -t/s$ , all factors  $1-z$  become unity in the high-energy limit. Thus,

$$\Gamma_{qg}^{(LL)}(\mu^2, \tilde{\mu}^2) = \frac{C_F}{C_A} \Gamma_{gg}^{(LL)}(\mu^2, \tilde{\mu}^2).$$

Simultaneously, due to the denominator part  $(1-z)$  in  $P_{qq}(z)$  quark production in the  $t$ -channel is suppressed, hence allowing to identify

$$\Gamma_q^{(LL)}(\mu^2, \tilde{\mu}^2) = \frac{C_F}{C_A} \Gamma_g^{(LL)}(\mu^2, \tilde{\mu}^2).$$

However,  $\Gamma_{qq}^{(LL)}(\mu^2, \tilde{\mu}^2)$  may be employed to model gluon emission from  $t$ -channel quark lines, as will be described in Sec. 5.

The above considerations show that to leading logarithmic accuracy the DUPDFs, Eq. (7), resemble all features of the BFKL evolution. Therefore, they can safely be employed as impact factors for the calculation of cross sections in the high-energy limit.

## 4 Markovian Monte Carlo solution to the $\ln(1/x)$ -evolution

The Markovian approach to the calculation of cross sections and differential distributions in the high-energy limit will be presented in this section. The advantage of the algorithm is that the number of emissions stays a priori undetermined, similar to the case of conventional parton showers employed to solve  $\log(Q^2/\mu^2)$ -evolution [45, 46, 47]. The factorisation of the radiation pattern into individual emissions, which depend on each other merely through the correct ordering, allows to model further physics effects involving the produced outgoing partons, like for instance adding final state radiation.

The basis of the formalism is encoded in Eq. (7) in [28] and Eq. (12). These equations translate into the probability for having an additional emission from the BFKL kernel being approximately distributed according to the function

$$\begin{aligned} \gamma(1, \Gamma_g^{(LL)}(y_i, y_n)) &= \Gamma_g^{(LL)}(y_i, y_n) \exp \left\{ -\Gamma_g^{(LL)}(y_i, y_n) \right\}. \end{aligned} \quad (14)$$

Here,  $y_i$  is the rapidity of the previous and  $y_n$  is the rapidity of the final emission. Such distributions may be generated employing the veto algorithm, described for example in [47]. It allows to simultaneously select the rapidity and transverse momentum of the new emission.<sup>7</sup> In the following, the superscripts  $(LL)$  will be dropped.

To determine the corresponding  $z$ - $k_{\perp}$ -factorisation formula, the simplest case, a gluon ladder with no emission, is investigated. This corresponds to a “ $2 \rightarrow 0$  process” in the  $z$ - $k_{\perp}$ -factorisation approach. When working in collinear factorisation rather than with the DUPDF prescription of [40], it is a  $2 \rightarrow 2$  process. The corresponding phase space element can thus be determined by factorising the collinear matrix element and its phase space integral. The starting point is

$$\begin{aligned} \sigma &= \sum_{a^{(1)}, a^{(2)}} \int d\xi^{(1)} \int d\xi^{(2)} \int \frac{d^4 k_1}{(2\pi)^3} \int \frac{d^4 k_2}{(2\pi)^3} \\ &\times \delta(k_1^2) \delta(k_2^2) (2\pi)^4 \delta^{(4)}(P - k_1 - k_2) \\ &\times f_{a^{(1)}}(x^{(1)}, Q^2) f_{a^{(2)}}(x^{(2)}, Q^2) \frac{|M_{a^{(1)} a^{(2)}}|^2}{2 \xi^{(1)} \xi^{(2)} S} \frac{1}{2}, \end{aligned} \quad (15)$$

where the factor  $1/2$  is due to the identity of the final state particles,  $Q^2$  denotes the factorisation scale,  $P^2 = s$ ,  $s = \xi^{(1)} \xi^{(2)} S$ ,  $\xi = x/z$ , and the superscripts  $(1)$  and  $(2)$  refer to the left and right beam, respectively. The matrix element reads

$$|M_{gg}|^2 = (4\pi\alpha_s)^2 \frac{C_A^2}{2} \left( 3 - \frac{tu}{s^2} - \frac{us}{t^2} - \frac{st}{u^2} \right). \quad (16)$$

Employing  $z_1 = z_2 = z$ ,  $t = -zs$  and  $u = -(1-z)s$  transforms this into

$$|M_{gg}|^2 = (4\pi\alpha_s)^2 \frac{1}{8} [P_{gg}(z)]^2 \{ 1 + \mathcal{O}(z(1-z)) \}$$

where terms proportional to  $z(1-z)$  in the numerator vanish in the high-energy limit and are not explicitly displayed.

The phase space element of the general case of a gluon ladder with an arbitrary number of gluons emitted between the two outermost jets can be derived by combining their momenta into one final state momentum  $K$ . Ignoring the substructure of  $K$ , the differential two-particle initial and final state phase space element for the remaining degrees of freedom reads

$$\begin{aligned} d\Phi_2 &= d\xi^{(1)} d\xi^{(2)} \frac{d^4 k_1}{(2\pi)^3} \frac{d^4 k_2}{(2\pi)^3} \delta(k_1^2) \delta(k_2^2) \\ &\times (2\pi)^4 \delta^{(4)}(P - K - k_1 - k_2), \end{aligned}$$

with  $P$  again the total four momentum of the process. Employing the four-dimensional  $\delta$ -function and the relations  $d\xi^{(1)} d\xi^{(2)} = dy ds/S$  and  $dp_z = d(\sqrt{s_{\perp}} \sinh y) =$

<sup>7</sup> In fact applying a veto is not necessary here, as long as quark production is neglected in the approach.

$\sqrt{s_\perp} \cosh y dy = E dy$  results in

$$d\Phi_2 = \frac{2\pi}{S} ds dy \frac{dy_1 dk_{1\perp}^2 d\phi_1}{4(2\pi)^3} \delta((P - K - k_1)^2) .$$

Furthermore, the definition  $\bar{P} = P - k_2$  allows to rewrite

$$\begin{aligned} \frac{dy}{dy_2} &= \frac{d}{dy_2} \frac{1}{2} \ln \frac{\bar{P}^+ + m_{2\perp} e^{+y_2}}{\bar{P}^- + m_{2\perp} e^{-y_2}} \\ &= \frac{1}{2} \left( \frac{m_{2\perp} e^{+y_2}}{P^+} + \frac{m_{2\perp} e^{-y_2}}{P^-} \right) = \frac{Pk_2}{s} . \end{aligned}$$

Using  $P = \sqrt{s} (\cosh y, \vec{0}, \sinh y)$  gives

$$\begin{aligned} ds \delta(s + K^2 - 2P(K + k_1) + 2Kk_1) \\ = \frac{s}{s - P(K + k_1)} = \frac{s}{Pk_2} , \end{aligned}$$

such that

$$d\Phi_2 = \frac{1}{4S(2\pi)^2} dy_2 dy_1 dk_{1\perp}^2 d\phi_1 .$$

Finally, when fixing the factorisation scale in Eq. (15) and the renormalisation scale in Eq. (16) to be the transverse momentum in the process and adding a Regge suppression factor for the  $t$ -channel gluon, the  $z$ - $k_\perp$ -factorisation formula reads

$$\begin{aligned} \sigma &= \frac{\pi^2}{2S} \int dy_1 \int dk_{1\perp}^2 \int d\phi_1 \int dy_2 \\ &\times \bar{f}_g(x^{(1)}, z, k_{1\perp}^2, \bar{k}_1^2) \bar{f}_g(x^{(2)}, z, k_{2\perp}^2, \bar{k}_2^2) \\ &\times \frac{1}{2\xi^{(1)2}\xi^{(2)2}S} \frac{1}{\bar{\Delta}_g(y_1, y_2)} . \end{aligned} \quad (17)$$

Here,  $\bar{f}_g$  is defined such that only gluon splittings are contained in the sum over parton species of Eq. (7) and angular ordering is implemented by the DUPDFs, while  $\bar{\Delta}_g(y_1, y_2)$  is given by Eq. (12). The superscripts  $(1)$  and  $(2)$  refer to the left and right beam, respectively. Since the emitted gluons are distinguishable due to rapidity ordering, the symmetry factor  $1/2$  appearing in Eq. (16) must be dropped. The factorisation scale  $\mu_F$  of each DUPDF introduced in Eq. (7) is unambiguously determined by the rescaled transverse momentum  $\bar{k}_\perp$  of the emissions.

Equation (17) describes a gluon ladder with no rung, but it can be easily extended to final states with an arbitrary number of gluons. In contrast to the previous case, the momentum fractions  $z^{(1)}$  and  $z^{(2)}$  are then generally different from each other. Hence we define the rescaled transverse momenta  $\bar{k}_{2\perp}^{(1)} = k_{2\perp}/(1 - z^{(1)})$  and  $\bar{k}_{n-1\perp}^{(2)} = k_{n-1\perp}/(1 - z^{(2)})$ . Employing Eq. (7) of [28], the

cross section for the  $2 \rightarrow n$  gluon scattering reads

$$\begin{aligned} \sigma &= \frac{\pi^2}{2S} \int dy_1 \int dk_{1\perp}^2 \int d\phi_1 \int dy_n \\ &\times \bar{f}_g(x^{(1)}, z^{(1)}, k_{1\perp}^2, \bar{k}_{2\perp}^{(1)2}) \bar{f}_g(x^{(2)}, z^{(2)}, k_{n\perp}^2, \bar{k}_{n-1\perp}^{(2)2}) \\ &\times \frac{1}{2\xi^{(1)2}\xi^{(2)2}S} \frac{1}{\bar{\Delta}_g(y_1, y_2)} \left[ \prod_{i=2}^{n-1} \int \frac{d\phi_i}{2\pi} \right. \\ &\times \left. \int dy_i \int \frac{dk_{i\perp}^2}{k_{i\perp}^2} \frac{\alpha_s(k_{i\perp}^2)}{\pi} C_{gg} \bar{\Delta}_g(y_i, y_{i-1}) \right] , \end{aligned} \quad (18)$$

where

$$C_{gg} = C_A .$$

The corresponding Monte Carlo event generation algorithm can be described as follows:

1. Determine the kinematics of the first emission and the rapidity of the last emission according to the modified  $z$ - $k_\perp$ -factorisation formula, Eq. (18).
2. As long as phase space allows, choose a new rapidity  $y_i$  according to Eq. (14) and a new transverse momentum  $k_{i\perp}$ . The corresponding cuts on the individual emissions have already been discussed in [28]. In the notation employed ibidem, they are given by

$$k_{i\perp}^2 > \mu_0^2 \quad \text{and} \quad q_{i\perp}^2 > \mu_0^2 .$$

3. Fix the transverse momentum of the last emission through overall momentum conservation.

## 5 Model for quark production

So far, it has been shown that Eq. (18) yields the correct LL gluon evolution in the high-energy limit. In this limit quark production is strongly suppressed due to the spin structure entering the corresponding vertices. However, energies and rapidity intervals at real colliders are finite and quarks do appear as final state partons. Since, for instance, heavy quark production is of large phenomenological interest, it needs to be described. In our approach we aim at not spoiling the high-energy gluon evolution. Therefore we choose to model quark production within the BFKL ladder structure by simply adding a  $g^*q^* \rightarrow q$  effective vertex, which vanishes in the high-energy limit, but keeping the finite, non-leading terms. Additionally, quarks can be produced by employing  $qg^* \rightarrow q$  and  $qq^* \rightarrow g$  impact factors contained within the DUPDFs. These quarks may further radiate gluons, which is modelled by a  $q^*q^* \rightarrow g$  vertex. Figure 2 shows a possible configuration of quark production.

Following Sec. 3, the remaining vertices are then readily determined. At leading logarithmic accuracy they are

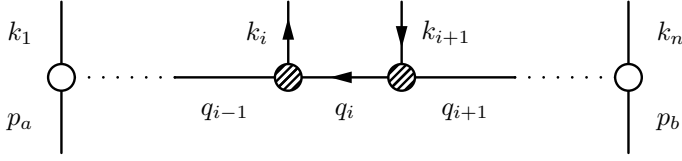


**Fig. 2** Multi-Regge amplitude including the emission of a quark pair with the particle indices  $i$  and  $i + 1$ . The shaded blobs represent the vertices proposed in Eq. (19).

given by the corresponding DGLAP splitting functions in the high-energy limit,

$$\begin{aligned} C_{qg} &= C_F, \\ C_{qq}(z_i) &= \frac{1}{2} C_F z_i, \\ C_{gq}(z_i) &= \frac{1}{2} T_R z_i. \end{aligned} \quad (19)$$

Then, the general case of a parton cascade in the high-energy limit reads

$$\begin{aligned} \sigma &= \frac{\pi^2}{2S} \sum_{a^{(1)}} \int dy_1 \int dk_{1\perp}^2 \int d\phi_1 \int dy_n \\ &\times f^{(1)}(x^{(1)}, z^{(1)}, k_{1\perp}^2, \bar{k}_{2\perp}^{(1)2}) f^{(2)}(x^{(2)}, z^{(2)}, k_{n\perp}^2, \bar{k}_{n-1\perp}^{(2)2}) \\ &\times \frac{1}{2\xi^{(1)2}\xi^{(2)2}S} \frac{1}{\Delta_{a_1}(y_1, y_2)} \left[ \prod_{i=2}^n \int \frac{d\phi_i}{2\pi} \int dy_i \int \frac{dk_{i\perp}^2}{k_{i\perp}^2} \right. \\ &\times \left. \frac{\alpha_s(k_{i\perp}^2)}{\pi} \sum_{a_i} C_{a_{i-1}a_i}(q_{i-1}, k_i) \Delta_{a_i}(y_i, y_{i-1}) \right], \end{aligned} \quad (20)$$

where now both quarks and gluons are contained in the sums over parton species.

If heavy quarks are included in the simulation, their masses are taken care of in the Reggeisation factor and the phase space integration. Following the discussion in [53], the branching probability  $\Gamma_Q^{(LL)}(y, \tilde{y})$  for heavy quarks of mass  $m$  is modified by

$$C_{qg} \longrightarrow \frac{k_{\perp}^2}{k_{\perp}^2 + m^2} C_{qg}. \quad (21)$$

Accordingly all external momenta are constructed employing the correct on-shell masses of the corresponding particles.

## 6 Results

In this section, results obtained with the Monte Carlo algorithm described above will be presented. All of them have been obtained with an implementation into the MC event generator Sherpa [54].<sup>8</sup> To eliminate possible dependencies on the phase space integration, we have

<sup>8</sup>This code is available from the authors upon request.

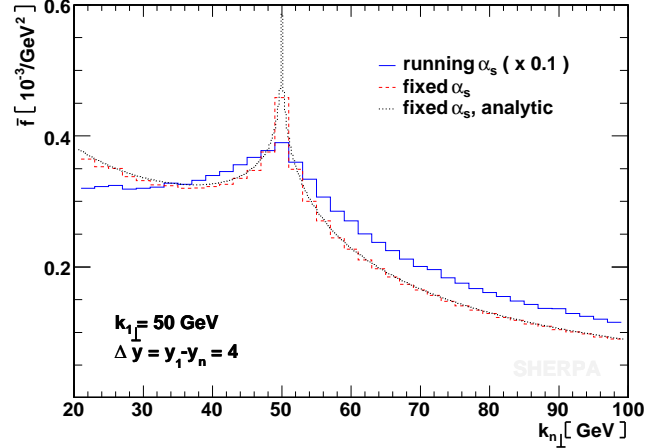


**Fig. 3** Transverse momentum spectra  $\bar{f}(k_{n\perp})$  for fixed and running coupling solution of Eq. (18) at fixed  $k_{1\perp}$  and  $\Delta y$ . Note that the result for running coupling has been rescaled by a factor of 0.1.

cross-checked our calculations with a different integration method. This method uses an iterative approach to generate event topologies for a fixed number of final state particles, as explained in the appendix. We found no deviations from our results generated in the Markovian approach.

Firstly, we focus on purely gluonic processes, reflecting the behaviour of the LO BFKL equation. This essentially translates into invoking Eq. (18) for event generation. In Fig. 3 the azimuthally averaged  $k_{n\perp}$  spectrum  $\bar{f}(k_{n\perp}) = \langle f(k_{n\perp}) \rangle_\phi$  is shown, where we have fixed  $k_{1\perp} = 50$  GeV and  $\Delta y = 4$ , and where the DUPDFs have been set to 1. Therefore, this plot investigates the behaviour of the BFKL kernel, Eq. (13), only. As collider setup, the LHC with a c.m. energy of 14 TeV has been chosen. In the fixed coupling solution  $\alpha_s$  has been evaluated at scale  $k_{1\perp}^2$ . The figure shows the effect of going from a fixed coupling and unconstrained kinematics to a running coupling with kinematical constraints, which considerably widens the distribution. Also, since  $\alpha_s$  is typically evaluated at smaller scales,  $\bar{f}$  is significantly enhanced. The large influence of kinematical constraints and running coupling on the BFKL dynamics has already been noted, e.g. in [32, 39].

As a next step, jet-production is investigated, comparing the results of the new algorithm to those obtained in collinear factorisation with on-shell matrix elements, which in the following will be denoted by DGLAP. The DGLAP results have been subject to the following corrections and constraints:

- ordering of final state momenta in rapidity,
- setting  $\mu_F^{(1)2} = k_{1\perp}^2$  and  $\mu_F^{(2)2} = k_{n\perp}^2$ ,
- evaluating the coupling weight as  $\prod_i \alpha_s(k_{i\perp}^2)$ .

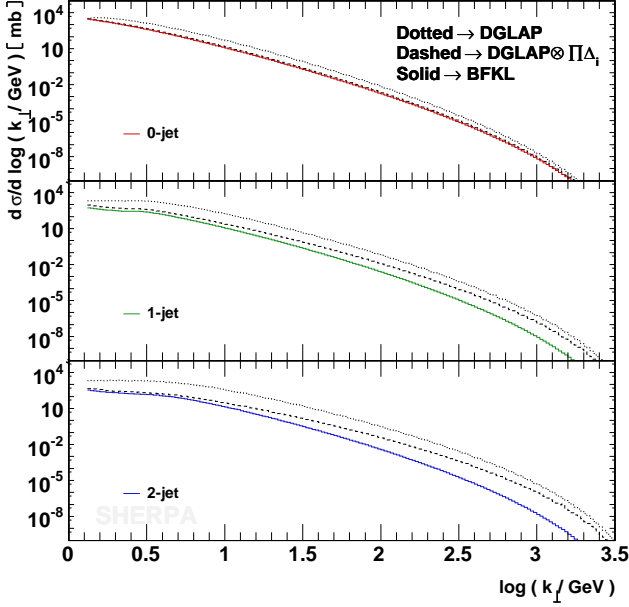


Fig. 4 Comparison of  $\log(k_\perp)$ -distributions between BFKL and reweighted DGLAP matrix elements.

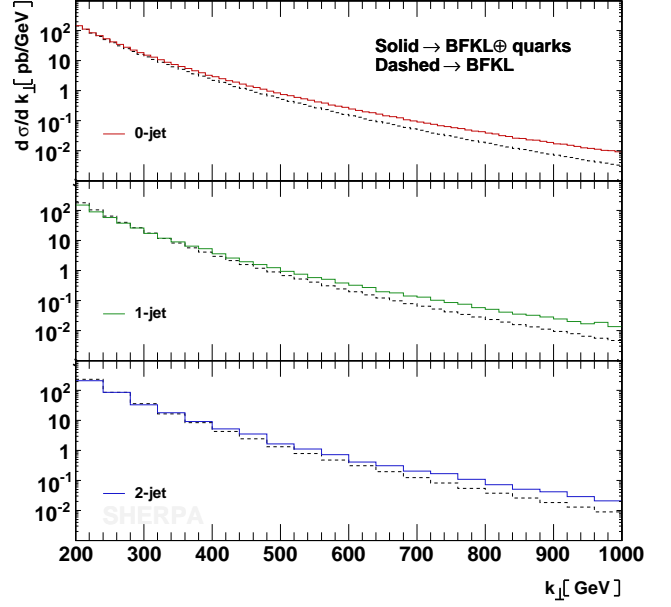


Fig. 6 Comparison of  $k_\perp$ -distributions between BFKL results with and without the inclusion of quarks in the simulation.

However, without any  $t$ -channel reggeisation factor in the DGLAP matrix elements there are still large differences. Applying a  $t$ -channel reggeisation weight to the DGLAP calculation results in much smaller discrepancies. The corresponding comparison for the  $\log(k_\perp)$ - and  $\Delta y$ -spectra is shown in Figs. 4 and 5. Due to the formal equivalence of Eqs. (15) and (17) at leading logarithmic accuracy, agree-

ment is to be expected and can be interpreted as another indication for the validity of the approach. Sizable deviations occur for  $k_\perp > 5$  GeV, which is due to the fact that the BFKL approach is bound to describe large energy partons only incompletely. In order to verify this, we have reweighted the BFKL matrix elements with the exact matrix element obtained in collinear factorisation. The corresponding correction weight for a  $2 \rightarrow n$  gluonic

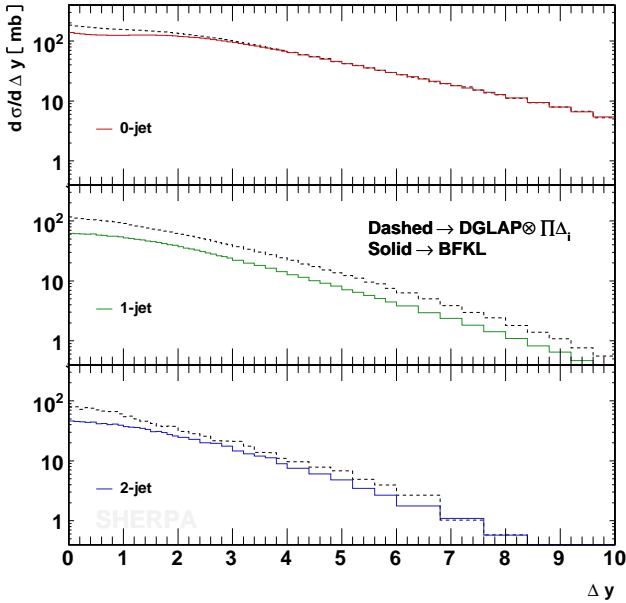


Fig. 5 Comparison between BFKL and reweighted DGLAP matrix elements for the  $\Delta y$ -distributions.

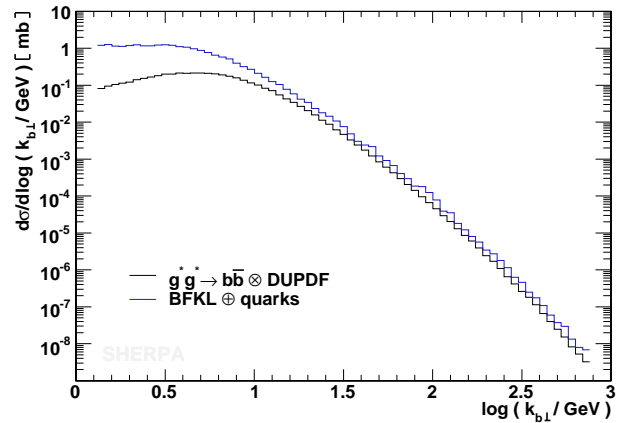


Fig. 7 Comparison of  $\log(k_{b,\perp})$ -spectra, calculated either using the matrix element given in [6] convoluted with DUPDFs or employing Eqs. (20) and (21).



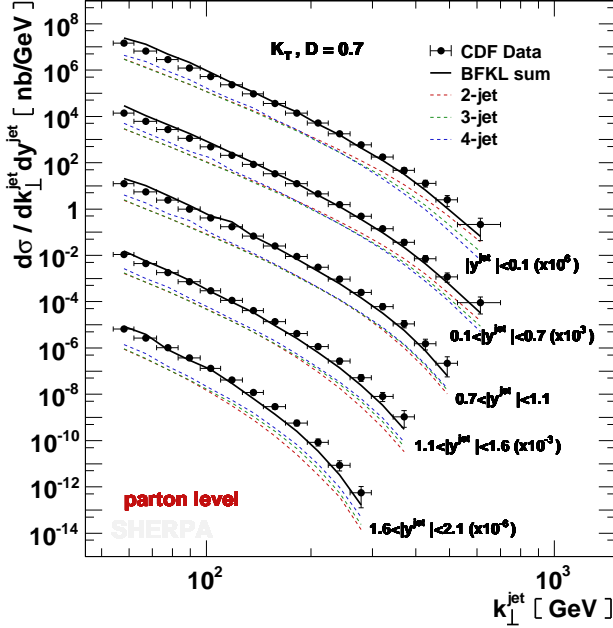


Fig. 8 Comparison of jet- $k_{\perp}$ -spectra with CDF data. Details of the analysis can be found in [55]. Dashed lines show contributions from subsamples of 2- to 4-particle final states.

process reads

$$\omega = \frac{8n! M_{gg \rightarrow ng}(1, \dots, n)}{(4\pi\alpha_s)^2 P_{gg}(z^{(1)})P_{gg}(z^{(2)}) \prod_{i=2}^{n-1} 16\pi^2 \bar{\alpha}_s/k_{i\perp}^2},$$

where the factor  $n!$  occurs due to the rapidity ordering in the BFKL approach and cancels the symmetrisation of the full DGLAP matrix element  $M_{gg \rightarrow ng}$ . Performing this reweighting yields exact agreement between the two approaches.

In a next step, all possible parton splittings in the DUPDFs as well as in the BFKL kernel have been enabled, i.e. Eq. (20) has been employed. As can be seen in Fig. 6, this results in a significant change of the  $k_{\perp}$ -spectra of the partons in the high- $k_{\perp}$  region, which is mainly due to the fact that quarks from the PDFs tend to have larger energies than the gluons. To examine the additional effect of heavy quark masses, we have compared our results to those obtained in high-energy factorisation along the lines of [6]. For this comparison we have used the full off-shell matrix element convoluted with DUPDFs. Figure 7 shows the  $\log(k_{\perp})$ -spectra of the heavy quarks in  $b\bar{b}$ -production. The coupling weight in the matrix element of the high-energy factorisation approach has been set to  $\alpha_s(k_{b\perp}^2)\alpha_s(k_{\bar{b}\perp}^2)$  in order to match the coupling weight in our approach. We obtain reasonable agreement with our calculation for  $k_{\perp} > 2m_b$ , where mass effects beyond Eq. (21) are expected to have less impact on the results.

Finally we have compared our results to recent experimental data. Firstly we show a comparison to data obtained by the CDF collaboration [55]. The corresponding pre-

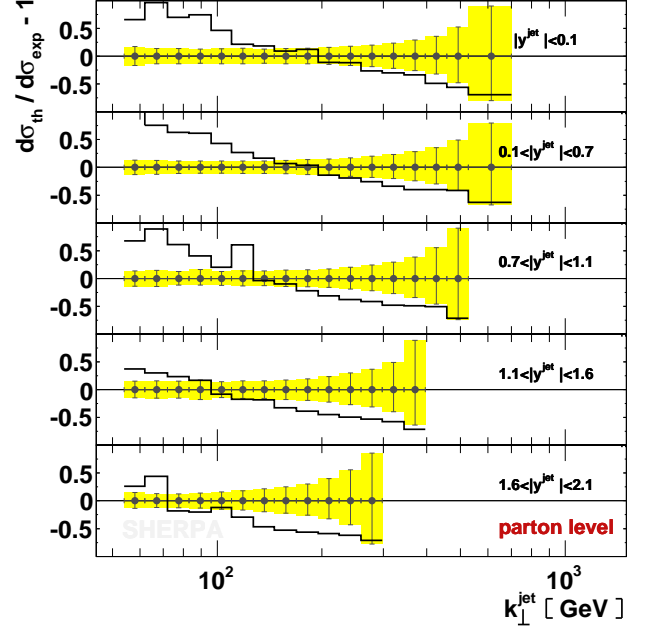


Fig. 9 Relative differences in jet- $k_{\perp}$ -spectra compared between the Monte Carlo results and CDF data in Fig. 8.

diction of jet- $k_{\perp}$ -spectra from our MC implementation is shown in Fig. 8. It fits the data considerably well, both in their shape and their normalisation. Note that no  $K$ -factor has been employed in the calculations. Although we observe a tilt of the distribution, which potentially arises from missing  $s$ -channel contributions to quark production, this is a quite remarkable result considering the fact that we employ a modified LO BFKL kernel for event generation. As can be seen in Fig. 9, deviations are up to  $\approx 50\%$ , which is well within the expected leading logarithmic accuracy.

Secondly we compare to the decorrelation observable investigated in Ref. [56]. As can be seen in Fig. 10 our approach does not completely describe the data. However, the deviations are of similar size as in Ref. [29]. We stress that the data have not been corrected to the parton level and therefore correlated and systematic errors might have an impact.

## 7 Conclusions

In this publication we have presented a new Monte Carlo algorithm for the description of particle production through the BFKL evolution equation. This has been achieved in a Markovian approach, iterating independent emissions in order to obtain the full BFKL radiation picture. It has been discussed how doubly unintegrated PDFs, obtained from conventional PDFs through the KMRW procedure can be employed as impact factors, retaining essential features of small- $x$  physics encoded in

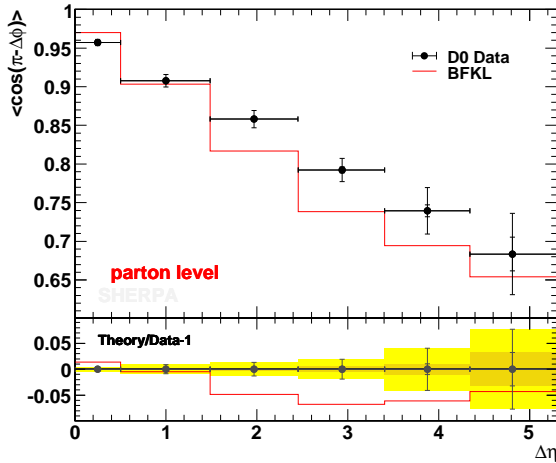


**Fig. 10** Comparison of the jet decorrelation observable presented in [56] with D0 data. The full error bars include both statistical and systematic errors, whereas statistical errors are independently highlighted by the smaller error bars.

the BFKL equation. In our opinion, this constitutes an important step towards a more unified event description, which allows to employ conventional PDFs deduced from global fits, rather than specialised parton distributions.

The implementation of this algorithm within the framework of a multi-purpose event generator has begun, and first results have been discussed. They indicate that the proposed algorithm correctly reproduces the BFKL features visible in analytical calculations as well as in other MC approaches. The results also show the important effect of a running of the coupling and of kinematical constraints, which go beyond the LO BFKL approach. The realisation of the Markovian algorithm is comparably straightforward. Using DUPDFs obtained from collinear PDFs allows to compare our results for jet production to those obtained in the collinear factorisation approach. We found that we can obtain good agreement between both approaches, even for multi-parton production, when effects that are not present in both approaches, such as  $t$ -channel reggeisation and rapidity ordering, are taken into account. In the same framework a model for quark production, which is beyond the LL approximation, has been included and its effect on jet production has been studied. Finally, we found that the new approach is capable to describe the production of high- $k_{\perp}$  jets at the Tevatron.

This work is a first step towards a unified description of particle production in the regime of high and low transverse momenta, i.e. of jet- and minijet-production. The formalism presented here can be extended to the simulation of multiple parton interactions, which constitute an important part of the underlying event. Also diffractive processes and quarkonia production may be included in the description.

## Acknowledgements

We like to thank A. D. Martin and M. G. Ryskin for fruitful discussions. We are especially grateful to J. R. Andersen for discussions concerning the treatment of running  $\alpha_s$  effects and his comments on the manuscript. SH thanks the HEPTOOLS Marie Curie RTN (contract number MRTN-CT-2006-035505) for an Early Stage Researcher position. TT thanks STFC (formerly PPARC) for an Advanced Fellowship. Financial support by MCNet (contract number MRTN-CT-2006-035606) and BMBF are acknowledged.

## A Alternative algorithm for phase space integration

We explain in this section a method to integrate over the  $n$ -particle phase space, which was employed to cross-check the algorithm presented in Sec. 4. We use an iterative approach to generate the event topology for the process  $p_a p_b \rightarrow p_1 \dots p_n$ . For each step in the iteration we consider a  $2 \rightarrow 2$ -scattering. Previous steps are taken into account by combining the particle momenta  $p_a, p_1 \dots p_i$  into  $p_{a_i}$  and thereby considering the  $2 \rightarrow 2$ -process  $p_{a_i} p_b \rightarrow p_i p_n$ . When denoting by  $s_i = m_i^2$  and  $s_{i\perp}$  the squared mass and squared transverse mass of the particle  $i$ , in the centre of mass frame of  $p_{a_i} p_b$  we obtain the integration boundaries

$$E_i^{\max} = \frac{1}{2m_{a_i b}} (s_{a_i b} + s_i - s_n) ,$$

$$k_{i\perp}^{\max} = \frac{1}{4s_{a_i b}} \lambda^2 (s_{a_i b}, s_i, s_n) ,$$

where  $\lambda^2 (s, s_1, s_2) = (s - s_1 - s_2)^2 - 4s_1 s_2$ . The corresponding rapidity interval is fixed by

$$y_i^{\max} = \frac{1}{2} \ln \frac{1 + \sqrt{1 - s_{i\perp}/E_i^{\max 2}}}{1 - \sqrt{1 - s_{i\perp}/E_i^{\max 2}}} ,$$

and may be computed once  $k_{i\perp}^2$  is selected. The  $k_{i\perp}^2$  selection is performed employing a divergence-free distribution, such as  $(k_{i\perp}^2)^\alpha$ , where  $\alpha > -1$ . Since the above boundaries are unambiguously determined, the  $n$ -particle phase space may be completely filled.

## References

- [1] J. C. Collins, D. E. Soper and G. Sterman, *Factorization of Hard Processes in QCD*, Adv. Ser. Direct. High Energy Phys. **5** (1988), 1–91, [hep-ph/0409313].
- [2] J. C. Collins, D. E. Soper and G. Sterman, *Soft gluons and factorization*, Nucl. Phys. **B308** (1988), 833–856.

- [3] A. D. Martin, R. G. Roberts, W. J. Stirling and R. S. Thorne, *Uncertainties of predictions from parton distributions. I: Experimental errors*, Eur. Phys. J. **C28** (2003), 455–473, [[hep-ph/0211080](#)].
- [4] A. D. Martin, R. G. Roberts, W. J. Stirling and R. S. Thorne, *Uncertainties of predictions from parton distributions. II: Theoretical errors*, Eur. Phys. J. **C35** (2004), 325–348, [[hep-ph/0308087](#)].
- [5] W. K. Tung et al., *Heavy Quark Mass Effects in Deep Inelastic Scattering and Global QCD Analysis*, JHEP **02** (2007), 053, [[hep-ph/0611254](#)].
- [6] S. Catani, M. Ciafaloni and F. Hautmann, *High Energy Factorization and Small- $x$  Heavy Flavour Production*, Nucl. Phys. **B366** (1991), 135–188.
- [7] J. C. Collins and R. K. Ellis, *Heavy quark production in very high energy hadron collisions*, Nucl. Phys. **B360** (1991), 3–30.
- [8] E. M. Levin, M. G. Ryskin, Y. M. Shabelski and A. G. Shuvaev, *Heavy Quark Production in Parton Model and in QCD*, Sov. J. Nucl. Phys. **54** (1991), 867–871.
- [9] P. Hägler, R. Kirschner, A. Schäfer, L. Szymanowski and O. V. Teryaev, *Direct  $J/\psi$  hadroproduction in  $k_T$ -factorization and the color octet mechanism*, Phys. Rev. **D63** (2001), 077501, [[hep-ph/0008316](#)].
- [10] A. V. Lipatov and N. P. Zotov, *Higgs boson production at hadron colliders in the  $k_T$ -factorization approach*, Eur. Phys. J. **C44** (2005), 559–566, [[hep-ph/0501172](#)].
- [11] A. V. Lipatov and N. P. Zotov, *Prompt photon photoproduction at HERA in the  $k_T$ -factorization approach*, Phys. Rev. **D72** (2005), 054002, [[hep-ph/0506044](#)].
- [12] M. G. Ryskin, A. G. Shuvaev and Y. M. Shabelski, *Charm hadroproduction in  $k_T$ -factorization approach*, Phys. Atom. Nucl. **64** (2001), 120–131, [[hep-ph/9907507](#)].
- [13] B. Andersson et al., *Small  $x$  Phenomenology: Summary and Status*, Eur. Phys. J. **C25** (2002), 77–101, [[hep-ph/0204115](#)].
- [14] E. A. Kuraev, L. N. Lipatov and V. S. Fadin, *The Pomeron Singularity in Nonabelian Gauge Theories*, Sov. Phys. JETP **45** (1977), 199–204.
- [15] I. I. Balitsky and L. N. Lipatov, *The Pomeron Singularity in Quantum Chromodynamics*, Sov. J. Nucl. Phys. **28** (1978), 822–829.
- [16] L. N. Lipatov, *Reggeization of the Vector Meson and the Vacuum Singularity in Nonabelian Gauge Theories*, Sov. J. Nucl. Phys. **23** (1976), 338–345.
- [17] B. Andersson, G. Gustafson and J. Samuelsson, *The linked dipole chain model for DIS*, Nucl. Phys. **B467** (1996), 443–478.
- [18] B. Andersson, G. Gustafson, H. Kharraziha and J. Samuelsson, *Structure functions and general final state properties in the linked dipole chain model*, Z. Phys. **C71** (1996), 613–624.
- [19] H. Kharraziha and L. Lönnblad, *The Linked Dipole Chain Monte Carlo*, JHEP **03** (1998), 006, [[hep-ph/9709424](#)].
- [20] M. Ciafaloni, *Coherence effects in initial jets at small  $Q^2/s$* , Nucl. Phys. **B296** (1988), 49–74.
- [21] S. Catani, F. Fiorani and G. Marchesini, *QCD coherence in initial state radiation*, Phys. Lett. **B234** (1990), 339–345.
- [22] S. Catani, F. Fiorani and G. Marchesini, *Small- $x$  behavior of initial state radiation in perturbative QCD*, Nucl. Phys. **B336** (1990), 18–85.
- [23] G. Marchesini and B. R. Webber, *Simulation of QCD initial state radiation at small  $x$* , Nucl. Phys. **B349** (1991), 617–634.
- [24] H. Jung and G. P. Salam, *Hadronic final state predictions from CCFM: The hadron-level Monte Carlo generator CASCADE*, Eur. Phys. J. **C19** (2001), 351–360, [[hep-ph/0012143](#)].
- [25] H. Jung, *The CCFM Monte Carlo generator CASCADE*, Comput. Phys. Commun. **143** (2002), 100–111, [[hep-ph/0109102](#)].
- [26] K. Golec-Biernat, S. Jadach, W. Płaczek, P. Stephens and M. Skrzypek, *Markovian Monte Carlo solutions of the one-loop CCFM equations*, Acta Phys. Polon. **B38** (2007), 3149–3168, [[hep-ph/0703317](#)].
- [27] J. Kwiecinski, C. A. M. Lewis and A. D. Martin, *Observable jets from the BFKL chain*, Phys. Rev. **D54** (1996), 6664–6673, [[hep-ph/9606375](#)].
- [28] C. R. Schmidt, *A Monte Carlo Solution to the BFKL Equation*, Phys. Rev. Lett. **78** (1997), 4531–4535, [[hep-ph/9612454](#)].
- [29] L. H. Orr and W. J. Stirling, *Dijet Production at Hadron-Hadron Colliders in the BFKL Approach*, Phys. Rev. **D56** (1997), 5875–5884, [[hep-ph/9706529](#)].
- [30] J. R. Andersen and A. Sabio-Vera, *Solving the BFKL Equation in the Next-to-Leading Approximation*, Phys. Lett. **B567** (2003), 116–124, [[hep-ph/0305236](#)].
- [31] J. R. Andersen and A. Sabio-Vera, *The Gluon Green’s Function in the BFKL Approach at Next-to-Leading Logarithmic Accuracy*, Nucl. Phys. **B679** (2004), 345–362, [[hep-ph/0309331](#)].
- [32] J. R. Andersen, *On the rôle of NLL corrections and Energy Conservation in the High Energy Evolution of QCD*, Phys. Lett. **B639** (2006), 290–293, [[hep-ph/0602182](#)].
- [33] J. R. Andersen, *The Quark-Antiquark Contribution to the Fully Exclusive BFKL Evolution at NLL Accuracy*, Phys. Rev. **D74** (2006), 114008, [[hep-ph/0611011](#)].
- [34] M. A. Kimber, A. D. Martin and M. G. Ryskin, *Unintegrated parton distributions and prompt photon hadroproduction*, Eur. Phys. J. **C12** (2000), 655–661, [[hep-ph/9911379](#)].

- [35] M. A. Kimber, A. D. Martin and M. G. Ryskin, *Unintegrated parton distributions*, Phys. Rev. **D63** (2001), 114027, [hep-ph/0101348].
- [36] G. Watt, A. D. Martin and M. G. Ryskin, *Unintegrated parton distributions and inclusive jet production at HERA*, Eur. Phys. J. **C31** (2003), 73–89, [hep-ph/0306169].
- [37] V. Del Duca and C. R. Schmidt, *BFKL versus  $\mathcal{O}(\alpha_s^3)$  Corrections to Large-rapidity Dijet Production*, Phys. Rev. **D51** (1995), 2150–2158, [hep-ph/9407359].
- [38] J. Kwieciński, A. D. Martin and P. J. Sutton, *Constraints on gluon evolution at small  $x$* , Z. Phys. **C71** (1996), 585–594, [hep-ph/9602320].
- [39] R. S. Thorne, *NLO BFKL Equation, Running Coupling and Renormalization Scales*, Phys. Rev. **D60** (1999), 054031, [hep-ph/9901331].
- [40] G. Watt, A. D. Martin and M. G. Ryskin, *Unintegrated parton distributions and electroweak boson production at hadron colliders*, Phys. Rev. **D70** (2004), 014012, [hep-ph/0309096].
- [41] G. Altarelli and G. Parisi, *Asymptotic freedom in parton language*, Nucl. Phys. **B126** (1977), 298–318.
- [42] L. N. Lipatov, *The parton model and perturbation theory*, Sov. J. Nucl. Phys. **20** (1975), 94–102.
- [43] V. N. Gribov and L. N. Lipatov, *Deep inelastic  $e$ - $p$  scattering in perturbation theory*, Sov. J. Nucl. Phys. **15** (1972), 438–450.
- [44] Y. L. Dokshitzer, *Calculation of the Structure Functions for Deep Inelastic Scattering and  $e^+e^-$  Annihilation by Perturbation Theory in Quantum Chromodynamics.*, Sov. Phys. JETP **46** (1977), 641–653.
- [45] R. D. Field, *Applications of perturbative QCD*, Addison-Wesley, Redwood City, USA, 1989, Frontiers in physics, 77.
- [46] R. K. Ellis, W. J. Stirling and B. R. Webber, *QCD and collider physics*, ed. 1, vol. 8, Cambridge Monogr. Part. Phys. Nucl. Phys. Cosmol., 1996.
- [47] T. Sjöstrand, L. Lönnblad, S. Mrenna and P. Skands, *PYTHIA 6.3 Physics and Manual*, hep-ph/0308153.
- [48] A. H. Mueller, *On the multiplicity of hadrons in QCD jets*, Phys. Lett. **B104** (1981), 161–164.
- [49] V. V. Sudakov, *Vertex parts at very high-energies in quantum electrodynamics*, Sov. Phys. JETP **3** (1956), 65–71.
- [50] G. Marchesini, *QCD coherence in the structure function and associated distributions at small  $x$* , Nucl. Phys. **B445** (1995), 49–80, [hep-ph/9412327].
- [51] L. V. Gribov, E. M. Levin and M. G. Ryskin, *Semi-hard Processes in QCD*, Phys. Rept. **100** (1983), 1–150.
- [52] V. del Duca, A. Frizzo and F. Maltoni, *Factorization of tree QCD amplitudes in the high-energy limit and in the collinear limit*, Nucl. Phys. **B568** (2000), 211–262, [hep-ph/9909464].
- [53] G. Rodrigo and F. Krauss, *Resummed jet rates for heavy quark production in  $e^+e^-$  annihilation*, Eur. Phys. J. **C33** (2004), 457–459, [hep-ph/0309325].
- [54] T. Gleisberg, S. Höche, F. Krauss, A. Schälicke, S. Schumann and J. Winter, *Sherpa 1.0, a proof-of-concept version*, JHEP **02** (2004), 056, [hep-ph/0311263].
- [55] A. Abulencia et al., *Measurement of the Inclusive Jet Cross Section using the  $k_T$  algorithm in  $p\bar{p}$  collisions at  $\sqrt{s} = 1.96$  TeV with the CDF II Detector*, Phys. Rev. **D75** (2007), 092006, [hep-ex/0701051], Erratum-ibid. **D75** (2007), 119901.
- [56] S. Abachi et al., *The Azimuthal Decorrelation of Jets Widely Separated in Rapidity*, Phys. Rev. Lett. **77** (1996), 595–600, [hep-ex/9603010].